IASS International Symposium '97 on Shell & Spatial Structures : 10 - 14 November 1997, Singapore

Wind Loading and Response of Large Stadium Roofs

J D Holmes, Monash University and JDH Consulting,, Australia
R Denoon, University of Queensland, Australia
K C S Kwok, University of Sydney, Australia
M J Glanville, Facade Technology Pty Ltd, Australia

ABSTRACT

Wind loading is usually the critical loading for the roofs of large fully- or partially-covered sports stadiums. The structure of these roofs could be of the space-frame, tensioned fabric or inflated type. As wind loading codes and standards do not cover such structures adequately, wind tunnel tests on models of the structure are usually commissioned for the purpose of providing wind loading information to designers. Two types of test have traditionally been carried out : aeroelastic models in which the mass and stiffness properties, as well as the aerodynamic shape, of the structure, are reproduced, and pressure measurements on simpler rigid models of the structure. The former type of test is expensive, and exact dynamic modelling may be difficult or impossible; also in practice all the wind loading information required by a designer is not obtained. Also for this type of structure, resonant dynamic response will not be a dominant part of the response. However, it *is* necessary to adequately include the dominant 'background' or sub-resonant fluctuating response in derivation of wind loads. A rigid pressure model has strong attractions, provided the appropriate treatment of the fluctuating pressures measured on such a model is carried out.

The paper describes a novel technique based on pressure measurements that has been adopted recently for two major Stadium roofs in Australia. In this technique, correlations of the fluctuating pressures on roof panels have been measured on wind-tunnel models, and used to produce effective or equivalent static wind loading distributions for the design of members in various parts of the structure. Peak deflections were also computed for various parts of the roofs.

For one of the structures, resonant contributions to both the equivalent load distributions and the deflections, for the first two modes of vibration, were included in the calculations. However these were relatively small contributions - of the order of 10% of the largest effective pressures and deflections.

J D Holmes, R Denoon, K C S Kwok, M J Glanville

1.0 INTRODUCTION

Wind loading is usually the critical loading for the roofs of large fully- or partially-covered sports stadiums. The structure of these roofs could be of the space-frame, tensioned fabric or inflated type. As wind loading codes and standards do not cover such structures adequately, wind tunnel tests on models of the structure are usually commissioned to provide wind loading information to designers.

Usually the information provided to designers by wind tunnels is in the form of wind loads or wind pressures, rather than load effects, such as bending moments, axial forces, reactions, etc. However, because wind flow and wind pressures are highly unsteady, varying in both time and space, there is usually not a simple relationship between local loads and load effects.

The fluctuations may excite resonant dynamic response if there is a resonant frequency low enough. In cases of some structures (such as long-span bridges), the resonant response in one or more modes may be dominant, in which cases, the inertial forces, distributed spatially according to the mode shapes, are the dominant fluctuating loads experienced by the structure. For structures which are not strongly resonant, such as the roofs of sports stadiums, there remains a component of fluctuating wind loading, sometimes called the 'background component' which affects the structure in a quasi-static way. There is no single spatial distribution for this fluctuating loading. The load distribution which produces the largest value of a structural load effect depends on the structural influence line for that load effect.

For sports stadiums, two types of wind-tunnel test have traditionally been carried out: aeroelastic modelling in which the mass and stiffness properties, as well as the aerodynamic shape, of the structure, are reproduced, and pressure measurements on simpler rigid models of the structure. The former type of test is expensive, and exact dynamic modelling may be difficult or impossible; also in practice all the wind loading information required by a designer is not obtained. Also for this type of structure, resonant dynamic response will not be a dominant part of the response. However, it *is* necessary to adequately include the dominant 'background' or sub-resonant fluctuating response in derivation of wind loads. A rigid pressure model has strong attractions, provided the appropriate treatment of the fluctuating pressures measured on such a model is carried out.

This paper describes a novel technique based on pressure measurements that has been adopted for two major Stadium roofs in Australia. In this technique, correlations of the fluctuating pressures on roof panels have been measured on wind-tunnel models, and used to produce effective or equivalent static wind loading distributions for the design of members in various parts of the structure. Peak deflections were also computed for various parts of the roofs.

2.0 THE STADIUM ROOFS

Stadium A (Figure 1) has an oval planform with fixed roofs on four sides, supported by large trusses. It also has a moving roof split in two halves, which in the fully closed position gives a totally enclosed arena. In the open position the moving roofs retract out over the fixed roofs on the east and west sides. The roof sections are nearly flat.

The roofs of Stadium B (Figure 2) are of hyperbolic paraboloid (saddle) shape on an oval planform, but open in the middle over the playing area. The two roofs are supported along the leading edges by space-frame arches.

3.0 WIND TUNNEL TESTS

Scale models of the proposed Stadiums, at geometric scaling ratios of 1/500 or 1/400, were constructed and installed in boundary-layer wind tunnels, in which boundary layers with characteristics appropriate to urban terrain were simulated. The turbulent boundary-layer flows were generated by a plain barrier spanning the start of the test section, followed by about 10 metres of small roughness blocks up to the models, which were mounted on a turntable.

In each case, basic wind pressure information was obtained from measurements on a number of panels on the top and bottom surfaces of each roof. Each panel pressure was obtained by pneumatically averaging the fluctuating pressures from up to ten individual pressure tappings. Specially designed pressure tubing systems enabling accurate measurements of the fluctuating panel pressures to a frequency of 200-300 Hertz on the model - equivalent to about 1-2 Hertz on the full-scale structures, were used.

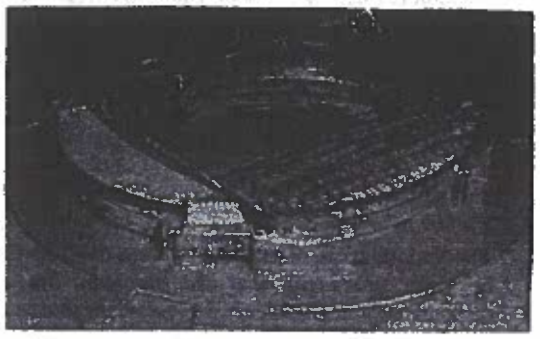

Figure 1. 1/400 scale Stadium A model

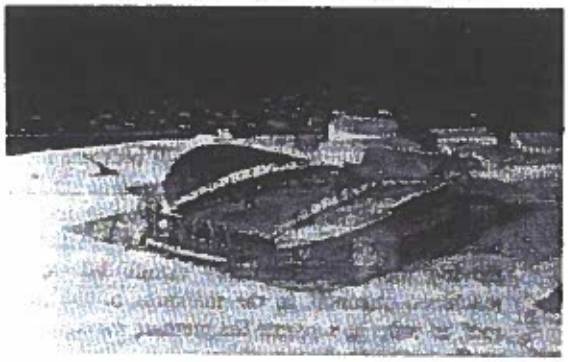

Figure 2. 1/500 scale Stadium B model.

4.0 BACKGROUND RESPONSE

The general approach to equivalent static wind loading distributions, including the mean (time-averaged), background fluctuating and resonant components, for various types of structures has been discussed by Holmes and Kasperski (1996).

To determine the background component of the loading the following procedure is adopted.

The complex time and spatially-varying wind pressure field on the roof for a given wind direction, can be divided into time varying parts $a_j(t)$, independent of spatial position, r, and spatially varying 'modes', e_{ij}, which depend on the spatial position, but are independent of time :

$$P_i(t) = \sum_j e_{ij}\, a_j(t) \qquad (1)$$

where j indicates the number of the mode. Note these are *not* the natural vibration modes of the roof - (see following section for discussion of the resonant dynamic response).

Various forms of orthogonal mode shapes e_{ij} could be chosen - e.g. for a hypar roof similar to Stadium B, but totally enclosing a stadium, a series of sine and cosine shapes were used [Davenport and Surry (1984)].

There are two important advantages in choosing the eigenvectors of the covariance matrix of the fluctuating pressures for the mode shapes [Holmes (1990)]:

a) the time series $a_j(t)$ are statistically uncorrelated with each other

b) only the first few modes (j = 1,2,....5 or 6) are required to accurately reproduce the original pressure field with the above equation.

However, it is not necessary to record time series of pressures to determine equivalent static loading distributions for the background response. For this, the approach of Kasperski and Niemann (1992) can be used.

Kasperski and Niemann give an equation for the pressure at a point, i, which corresponds to the maximum value of a load effect, X, such as bending moment or member force :

$$(p_i)_X = \bar{p}_i + g_X\, r_{p_i X}\, \sigma_p \qquad (2)$$

where $\bar{p}_i$ is the mean pressure at i
g_X is a peak factor (in the range of 2.5 to 5)
$r_{p_i X}$ is the correlation coefficient between p_i and X
σ_p is the r.m.s. fluctuating pressure at i

Calculation of $r_{p_i X}$ requires the influence coefficients for X, as well as the correlations between all the fluctuating pressures on the roof. In its original form [Kasperski and Niemann (1992)], the calculations of $(p_i)_X$ involve double integrations, or summations, and are fairly complex, requiring computer programs. However in a modified form [Holmes (1992)], when the decomposition into the eigenvector modes described previously is used, the calculations only involve single summations and can be carried out on a Spreadsheet, such as EXCEL. Once the Spreadsheets are set up it is very easy to incorporate the influence coefficients for new load effects.

The results of these calculations produce equivalent static loading distributions for each of the specified load effects, which can be represented as linear combinations of the first few eigenvector modes. This allows generally applicable load distributions to be proposed and used by the structural designers as static loads in a structural analysis package to design all the members in the structure.

5.0 RESONANT RESPONSE

If the lowest natural frequencies of a roof are less than 1 Hertz, a small amount of resonant dynamic response in a roof could be expected. This may be calculated by weighting recorded time series of the panel pressures by the mode shapes for the significant modes.

The modal-weighted pressures are then spectrally analysed to determine the spectral density of each modal force around the natural frequency of each mode. Then calculation of the deflection and acceleration response is fairly straightforward using random vibration theory, as described in the Appendix.

The equivalent static load distribution for the resonant loading is the peak inertial loading due to the vibrating structure, and is independent of load effect. This can be calculated for each mode of vibration from the accelerations, and combined with the background distributions with a root-sum-of-squares approximation. The calculation of the inertial contribution is described in the Appendix.

6.0 COMBINATION OF LOADING CONTRIBUTIONS

To combine the resonant loading (assuming two modes of vibration are important) with the background response, a 'root sum of squares' rule can be applied :

$$p_{eff} \cong \bar{p} \pm \sqrt{[p_B^2 + p_{R,1}^2 + p_{R,2}^2]} \quad (3)$$

where p_{eff} is the total effective peak pressure

$\bar{p}$ is the mean pressure

p_B is the peak background component (peak - mean)

$p_{R,1}$ is the peak resonant (inertial) pressure in mode 1

$p_{R,2}$ is the peak resonant (inertial) pressure in mode 2

Equation (3) assumes that the background component and the two resonant components are uncorrelated with each other. The positive root is taken if p_B is positive and vice-versa.

Equation (3) may need modification for load effects with influence lines changing sign across a roof, coinciding with resonant modes with changing sign.

7.0 TEST CASES

7.1 Stadium A

The various roofs of stadium A were considered to be sufficiently stiff that the resonant dynamic response was negligible. 16 pressure measurement panels were provided on the fixed West roof, and 12 on the fixed North roof. In both cases, two panels were provided for the underside of the roofs. The loads on the fixed East and South roofs were obtained from the West and North roofs, by symmetry. One half of the moving roof was also covered with 14 upper surface panels and 2 underneath.

In order to minimise the amount of pressure tubing under the moving roof in the open position (and thus allow free flow of air between the moving roof and the fixed roof underneath), the pressure panels of the moving roof were internally manifolded through machined channels in the thickness of the model roof, in order to separate the pressure measurements on the top and bottom surfaces.

Nearly simultaneous pressure sensing was carried out for each instrumented roof using an electronic pressure scanner (ZOC-16 scanner from Scanivalve Corporation). In-house software on a PC enabled the mean, r.m.s. and peak pressure coefficients to be determined. In addition, all the correlation coefficients for every pair of panels within a single roof were calculated. This information enabled the effective static load distributions and peak load effects, to be determined. Measurements were carried out for a variety of different open roof configurations, and for sixteen different wind directions.

An example of a correlation matrix is given in Table I. A value of 1.0 indicates fully correlated (or synchronised) pressure fluctuations; lesser values indicate lower correlation. Generally, higher values of correlation coefficient occur for pairs of adjacent panels, than for well-separated panels. Design codes and standards usually assume full correlation for pressures on the same surface (this is known as the 'quasi-steady' assumption) - however this results in conservative loadings for large roofs. The methodology described in this paper allows designers to take advantage of the reduced loadings generated by the partially correlated pressure fluctuations.

Table I. Correlation matrix for North Roof of Stadium A

Panel	1	2	3	4	5	6	7	8	9	10	11	12
1	1	0.72	0.72	0.51	0.54	0.52	0.45	0.49	0.32	0.22	0.64	0.69
2	0.72	1	0.64	0.75	0.70	0.66	0.63	0.62	0.50	0.41	0.67	0.67
3	0.72	0.64	1	0.43	0.75	0.42	0.55	0.44	0.38	0.22	0.63	0.65
4	0.51	0.75	0.43	1	0.67	0.84	0.7	0.69	0.6	0.54	0.61	0.57
5	0.54	0.70	0.75	0.67	1	0.62	0.83	0.60	0.61	0.41	0.67	0.62
6	0.52	0.66	0.42	0.84	0.62	1	0.73	0.84	0.67	0.59	0.69	0.65
7	0.45	0.63	0.55	0.7	0.83	0.73	1	0.71	0.79	0.56	0.65	0.58
8	0.49	0.62	0.44	0.69	0.60	0.84	0.71	1	0.73	0.7	0.75	0.71
9	0.32	0.50	0.38	0.6	0.61	0.67	0.79	0.73	1	0.74	0.53	0.48
10	0.22	0.41	0.22	0.54	0.41	0.59	0.56	0.7	0.74	1	0.37	0.37
11	0.64	0.67	0.63	0.61	0.67	0.69	0.65	0.75	0.53	0.37	1	0.92
12	0.69	0.67	0.65	0.57	0.62	0.65	0.58	0.71	0.48	0.37	0.92	1

The methodology described in Section 4.0 enables the peak (expected maximum and minimum values) and the corresponding effective static loading distributions to be determined for any load effect for which the influence coefficients are available.

Examples of influence coefficients for a deflection and for an axial force in the top chord member of the main truss supporting the West roof are given in Table II. These values represent the deflection or truss force, as a uniformly distributed panel load of unit magnitude is applied in turn to every pressure panel on the roof.

The variations of these two load effects under wind load, as the wind direction varies, as calculated by the method described in Section 4.0, are shown in Figure 3. The calculations have allowed for the non-uniform variation of design wind speed with direction at the site of the Stadium, and this variation has been incorporated into Figure 3. For one wind direction, the effective static load distributions corresponding to the deflection and the truss force are shown in Figure 4. In this Figure, they are compared with the recorded maximum panel pressures. The lower values obtained by the present methodology indicates the reductions produced by the partial correlation of the fluctuating pressures (e.g. Table I).

Table II. Influence coefficients for a deflection and a truss force (West roof -Stadium A)

Loaded Panel	Influence Coefficient for deflection at Panel 8 (mm)	Influence Coefficient for top chord truss force (kN)
1	6.1	580
2	2.1	331
3	-0.1	70
4	111.9	2705
5	68.1	1760
6	28.1	770
7	1.6	37
8	281.3	1872
9	140.4	1210
10	39.5	533
11	0.9	28
12	91.6	367
13	49.9	184
14	11.1	418
15	-614.7	-4612
16	-217.7	-6253

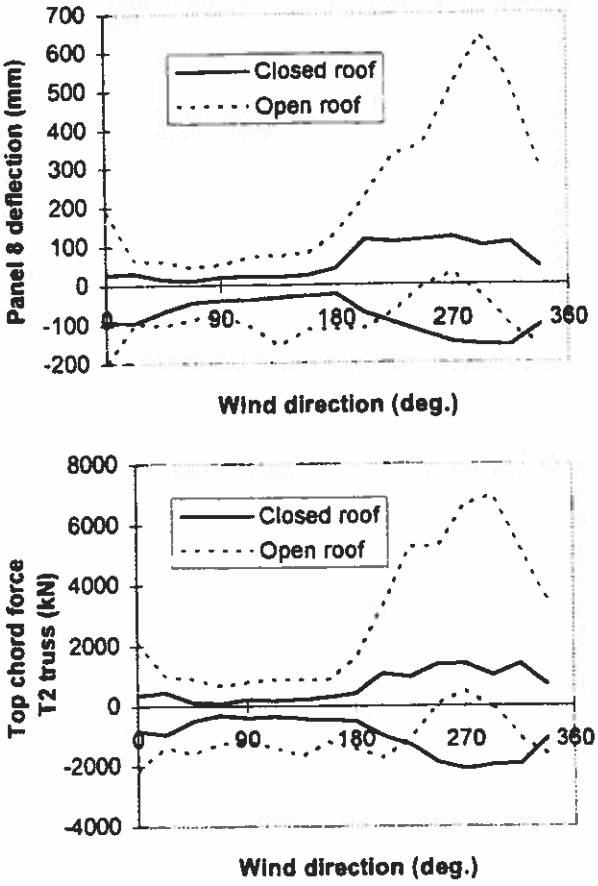

Figure 3. Variation of a deflection and a truss force with wind direction (West Roof - Stadium A)

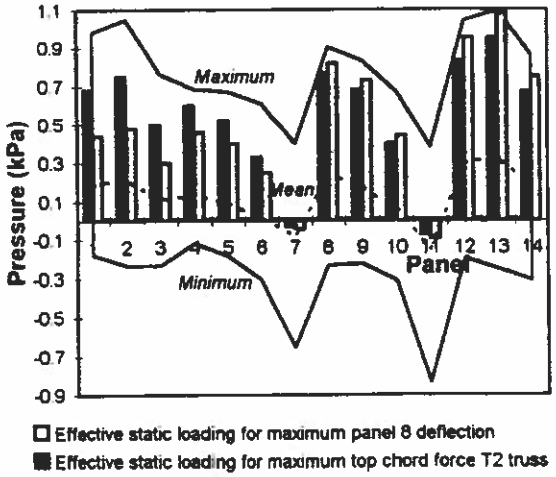

Figure 4. Effective static loading distributions for West Roof of Stadium A

7.2 Stadium B

Figure 5 shows the panel arrangement. for the roofs of this Stadium. 25 panels (including one underneath) were used. with up to four individual pressure tappings within each panel being manifolded together to give the fluctuating panel pressures. Each manifolded panel pressure was measured by a Honeywell 163 pressure sensor, whose outputs were sampled by analog-digital converters controlled by two personal computers.

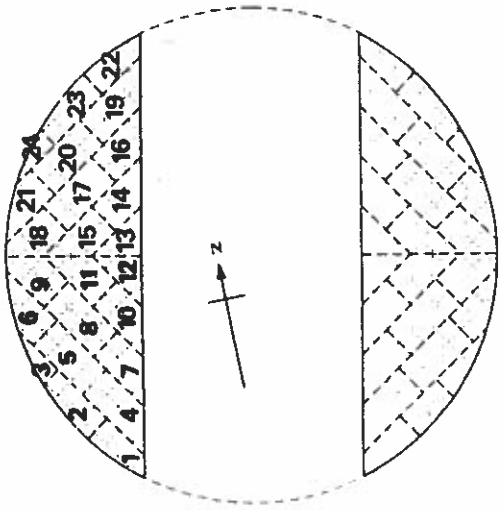

Figure 5. Panel numbering system for Stadium B.

As for Stadium A. the mean and standard deviation of the individual panel pressures (and the corresponding pressure coefficients) were obtained. together with the correlation coefficients of the fluctuating pressures for every pair of panels. for wind directions at 22.5 degree intervals. However, in addition for this study, time histories of the panel pressures (including 1 panel for the underside roof pressure) were recorded simultaneously and stored on computer disk. These were required to determine the small amount of resonant response. in the two lowest modes. with frequencies of 0.64 and 0.73 Hertz (as discussed in Section 5.0 and the Appendix).

An example of the effective load distribution calculated for the truss forces in the central part of the main arch West Roof of Stadium B is given in Figure 6. This distribution has been shown with and without the resonant contributions included. As can be seen the resonant contributions are small.

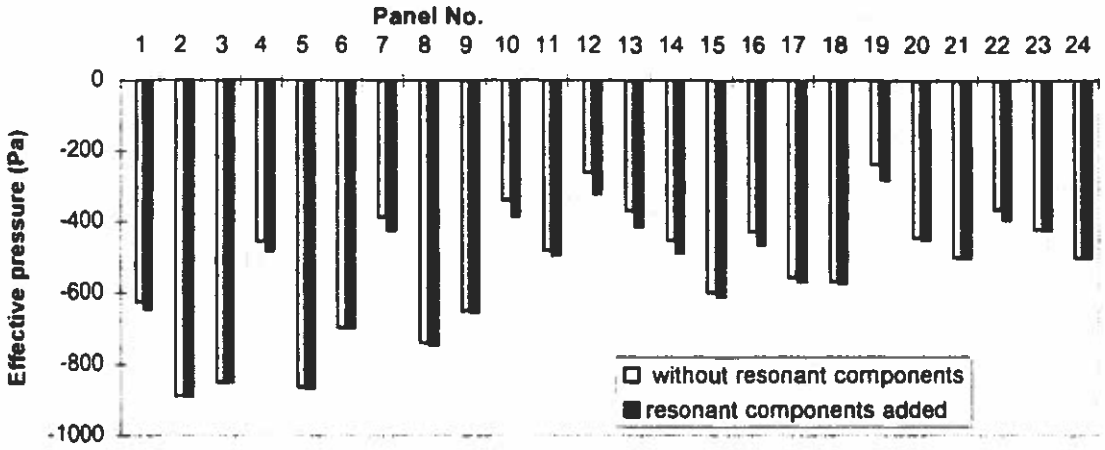

Figure 6. Effective load distributions for Stadium B (Arch truss forces - West roof -WSW wind)

The peak deflections at the centres of the panels were also predicted for this Stadium, and are shown for the West Roof in Figure 7 (for an exceedence probability of 5% in any year). Three different levels of damping were assumed. Figure 7 shows that the assumed damping level has little effect, as the resonant components are not large contributions to the overall peak deflections.

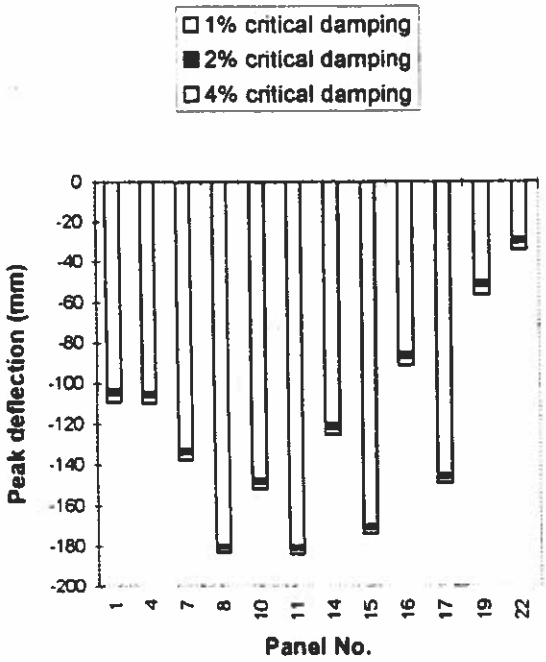

Figure 7. Peak deflections on West roof of Stadium B (WSW wind)

8.0 CONCLUSIONS

This paper has described a novel state-of-the-art technique for the determination of wind loads, based on pressure measurements, that has been adopted recently for two major Stadium roofs in Australia. In this technique, correlations of the fluctuating pressures on roof panels have been measured on wind-tunnel models, and used to produce effective or equivalent static wind loading distributions for the design of members in various parts of the structure. Peak deflections were also computed for various parts of the roofs.

For one of the structures, resonant contributions to deflections, for the first two modes of vibration, were included in the calculations. However these were relatively small contributions - of the order of 10% of the largest effective pressures and deflections.

This technique requires relatively simple wind-tunnel models, and enables all the information required by structural designers to be obtained.

9.0 REFERENCES

Davenport, A G and Surry, D - Turbulent wind forces on a large span roof and their representation by equivalent static loads. *Canadian Journal of Civil Engineering*, Vol. 11, pp 955-966, 1984.

Holmes, J D - Analysis and synthesis of pressure fluctuations on bluff bodies using eigenvectors. *Journal of Wind Engineering and Industrial Aerodynamics*, Vol. 33, pp 219-230, 1990.

Holmes, J D - Optimised peak load distributions. *Journal of Wind Engineering and Industrial Aerodynamics*. Vol. 41. pp 267-276. 1992.

Holmes, J D and Kasperski, M - Effective distributions of fluctuating and dynamic wind loads. *Civil and Structural Engineering Transactions, Institution of Engineers, Australia*. Vol. CE38. pp 83-88. 1996.

Kasperski, M and Niemann, H-J - The L.R.C. (Load-response-correlation) Method - A general method of estimating unfavourable wind load distributions for linear and non-linear structural behaviour. *Journal of Wind Engineering and Industrial Aerodynamics*. Vol. 43. pp 1753-1763. 1992.

APPENDIX - CALCULATION OF RESONANT RESPONSE, AND CONTRIBUTION TO EFFECTIVE STATIC LOADING

For low damping ratios, the mean square resonant generalised coordinate for the jth mode of vibration can be adequately approximated by :

$$\sigma_{aj}^2 = [\pi\, n_j\, S_{Fj}(n_j)] / [4\, K_j^2 \zeta_j] \qquad (A1)$$

where a_j is the generalised coordinate for the jth mode of vibration ; n_j is the natural frequency of the jth mode (Hertz); K_j is the generalised stiffness equal to $(\omega_j^2\, G_j)$

ω_j (= $2\pi\, n_j$) is the circular frequency

G_j is the generalised mass

ζ_j is the critical damping ratio for the jth mode

The mean square deflection due to resonance in the jth mode at any point, i, on the roof is then given by:

$$\sigma_z^2 = \mu_{ij}^2\, \sigma_{aj}^2 = \mu_{ij}^2\, [\pi\, n_j\, S_{Fj}(n_j)] / [4\, K_j^2\, \zeta_j] \qquad (A2)$$

The mean square acceleration at i is, to a good approximation :

$$\omega_j^4\, \sigma_z^2 = \mu_{ij}^2\, [\pi\, n_j\, S_{Fj}(n_j)] / [4\, G_j^2\, \zeta_j] \qquad (A3)$$

Finally the peak inertial force at each panel, i, is given by:

$$F_I = g_j\, m_i\, \mu_{ij}\, \sqrt{\{[\pi\, n_j\, S_{Fj}(n_j)] / [4 G_j^2\, \zeta_j]\}} \qquad (A4)$$

where g_j is a peak factor given by

$g_j = \sqrt{(2 \log_e n_j T)} + 0.5772 / \sqrt{(2 \log_e n_j T)}$

and m_i is the mass of the panel i. T is an appropriate time period such as 10 minutes or 1 hour.

Equation (A4) can be written more conveniently in the form :

$$F_I = g_j\, [m_i\, \mu_{ij} / \Sigma\, m_i\, \mu_{ij}^2]\, (\sigma_{Fj} / \bar{F}_j)\, \bar{F}_j \sqrt{\{\pi\, [n_j\, S_{Fj}(n_j) / \sigma_{Fj}^2] / [4\, \zeta_j]\}} \qquad (A5)$$

where $\bar{F}_j$ is the mean generalised force in the jth mode and σ_{Fj} is the standard deviation of the generalised force.

An equivalent pressure can be obtained by dividing by the area of the panel.

The terms $(\sigma_{Fj} / \bar{F}_j)$ and $[n_j\, S_{Fj}(n_j) / \sigma_{Fj}^2]$ are respectively, the 'intensity' of the modal force, and the normalised spectral density evaluated at the natural frequency n_j. They were obtained by weighting the recorded time series of the panel pressures by the mode shape coordinate μ_{ij} (and the area of the panel) and summing to form a time series of the generalised force $F_j(t)$, and then computing the mean, standard deviation and normalised spectral density.

ACKNOWLEDGEMENTS

The authors acknowledge the cooperation of Consulting Engineers, Modus (U.K.) and Connell Wagner (Australia) during the wind studies for Stadiums A and B, the programming skills of Malcolm Macleod (Monash University) and Dan Popovich (University of Sydney), and the advice of Professor W.H. Melbourne (Monash University).